International Journal of Control, Automation and Systems 18(7) (2020) 1651-1661
http://dx.doi.org/10.1007/s12555-019-0987-3
ISSN:1598-6446 eISSN:2005-4092
http://www.springer.com/12555

# Model Reference Robust Adaptive Control of Control Element Drive Mechanism in a Nuclear Power Plant

**Bae-Jeong Park, Phuong-Tung Pham, and Keum-Shik Hong***

**Abstract:** In the nuclear power plant, the control element drive mechanism (CEDM: A type of solenoid actuators) is used to insert nuclear fuel rods into the core to regulate the neutron absorption within the reactor. The control environment is full of uncertainty and disturbance, and the CEDM is supposed to cope with the varying conditions in the reactor. In this paper, a model reference adaptive control (MRAC) of CEDM is investigated. The existing MRAC scheme that assumes the known system order is first extended to the system with unknown high-frequency gain and output disturbance, and then the extended version is applied to the control problem of CEDM. A simplified relationship between the input voltage and the magnetic force of the CEDM is established based on Kirchhoff's voltage law and the magnetic co-energy theory. The system order of the plant is identified by the prediction error method using experimental input/output data: A 3rd order linear model with three poles and two zeros turns out to be the best model for control. Based on this model, a 3rd order reference model is selected, and an adaptive control law with $\sigma$-modified adaptation laws is designed under output disturbance. The performance of the proposed control law is compared with a well-tuned PI controller and the conventional MRAC. The superiority of the proposed method is also demonstrated in an abnormal condition. Simulation and experiment results are provided.

**Keywords:** Control element drive mechanism, model reference adaptive control, nuclear power plant, solenoid, system identification.

## 1. INTRODUCTION

In the nuclear power plant, nuclear fuel rods (i.e., control rods) are inserted into the reactor core to alter the neutron absorption and control the nuclear reaction rate. In this process, the level of insertion is regulated by a control element drive mechanism (CEDM) (also called the control rod drive mechanism) [1]. The CEDM consists of a drive-shaft assembly carrying fuel rods, electromagnetic coil assemblies (i.e., the upper/lower lift and gripper coils), and latch mechanisms, see Fig. 1. The coil assemblies are solenoid actuators that move and hold the drive-shaft. The CEDM governs the insertion and withdrawal of control rods by energizing and de-energizing the electromagnetic coils of solenoid actuators. In the nuclear industry, the safety and robust control in the presence of uncertainty and disturbance is most crucial [2, 3]. In this paper, a model reference adaptive control to cope with parametric uncertainties and the presence of output disturbance is investigated.

The CEDM has complicated dynamic characteristics owing to the assembly nature of mechanical, electrical, and magnetic elements. Several studies on the development of a CEDM were performed [4–7]: Ishida and coworkers presented a compact CEDM for the reactor vessel of the advanced marine reactor MRX [4]. In Yoritsune *et al.* [5], a novel latching assembly using a magnetic force was developed for small reactors. Concerning the electromagnetic characteristics of the CEDM, Kim *et al.* [8] used a finite element method to analyze electromagnetic effects and then calculated the latching force of the CEDM in the APR-1400 nuclear reactor. Lee *et al.* [9] experimentally investigated the characteristics of the solenoid actuator of the CEDM in the APR-1400 nuclear reactor. Subsequently, Lee *et al.* [7] developed an optimized design of the nonmagnetic motor housing based on a finite element electromagnetic analysis.

In the CEDM, the solenoid actuator is an essential element that generates the latching force for the latch mechanism through energizing/de-energizing processes of the electromagnetic coils (Fig. 2). Owing to their broad applications, the dynamics and control of solenoid actuators have been extensively studied. The linear and nonlinear dynamic models of the solenoid actuator were pre-

Manuscript received November 25, 2019; revised February 11, 2020; accepted February 18, 2020. Recommended by Editor Fumitoshi Matsuno. This work was supported by a Two-Year Research Grant of Pusan National University.

Bae-Jeong Park is with the Nuclear Power (BG) Control Systems Design Team, Doosan Heavy Industries and Construction, 37 Samsung 1-ro 5-gil, Hwaseong-si, Gyeonggi-do 18449, Korea (e-mail: baejeong.park@doosan.com). Phuong-Tung Pham and Keum-Shik Hong are with the School of Mechanical Engineering, Pusan National University, 2 Busandaehak-ro, Geumjeong-gu, Busan 46241, Korea (e-mails: {pptung, kshong}@pusan.ac.kr).
* Corresponding author.

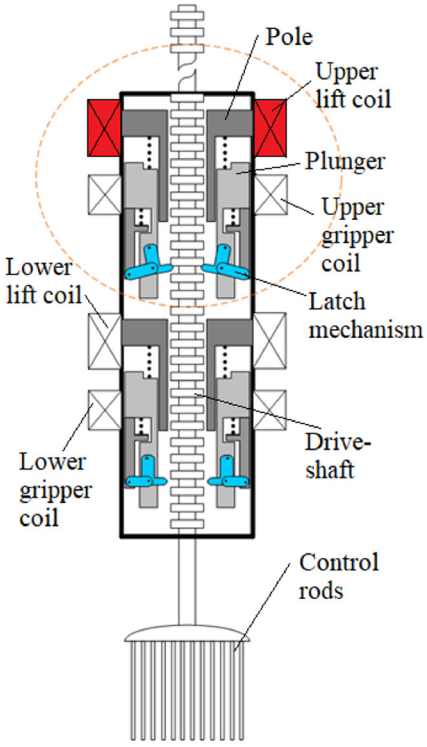


Fig. 1. Latch-type control element drive mechanism.

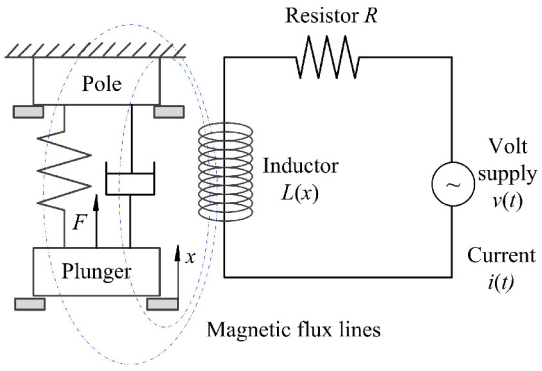


Fig. 2. Solenoid system in a latch-type CEDM.

sented in Vaughan and Gamble [10]. Later, various investigations to establish models for modified solenoid actuators and validating their performance have been conducted [11–13]. Control strategies of solenoid actuators were also developed in [14–18]. Rahman *et al.* [14] presented a position estimation method using the relationship between the position, incremental inductance, and the current of a solenoid actuator, whereas Ronchi *et al.* [16] estimated the plunger position using the flux analysis. In [17], the impact velocity of the plunger and valve of a solenoid system was controlled using a nonlinear flatness-based estimated state feedback control. Eyabi and Washington [19] proposed a nonlinear sensorless sliding mode estimate approach and then designed a closed-loop nonlinear controller based on the estimated parameter. In their work, the robust control design was used to compensate for the influence of the hysteresis and saturation effects due to losses in the magnetic core. In [20], a sensorless robust position control scheme for compact solenoid actuators was proposed, and then its performance was verified experimentally.

Thus far, to the best of our knowledge, studies on the control of the solenoid actuator in the presence of unknown parameters and disturbances in the reactor are limited. In Fig. 2, the entire system consists of two parts: An electrical circuit and a mechanical mass-spring-damper system. The output in the electrical part is the inductor current, while that in the mechanical part is the plunger displacement. Output disturbances in the electrical subsystem include temperature variation in the reactor, degradation of electrical components, etc., and those in the mechanical subsystem are sensor deterioration, gear backlash, water swirling, etc. In this paper, disturbances are assumed in sinusoidal forms.

In this paper, adaptive control of a solenoid actuator in the latch-type CEDM in the nuclear power plant industry is investigated. First, the governing equation of the solenoid actuator is developed using Kirchhoff's voltage law and the magnetic co-energy theory. According to the experimental input/output data, identification of unknown parameters appearing in the system model is performed by assuming that the structure of the mathematical model is known. Subsequently, a robust model reference adaptive control is developed for the system in the presence of unknown parameters and output disturbance. Furthermore, the performance of the proposed control law is verified through simulation and experimental data.

This paper is organized as follows: Section 2 provides a modified model reference adaptive control (MRAC) algorithm for the n-th order linear system with output disturbance. In Section 3, dynamical models of the solenoid actuator in the CEDM obtained by i) a simplified theoretical approach and ii) a system identification approach and the adaptive control law are developed. Section 4 presents the simulation results. Section 5 describes the experimental results. Finally, conclusions are drawn in Section 6.

## 2. MODIFIED MODEL REFERENCE ADAPTIVE CONTROL

Adaptive control is a powerful approach that can handle the system with uncertainties [21–23]. It was extensively implemented in diverse systems [24–37]. An output-feedback adaptive control for linear systems with unknown coefficients was well developed in [38], in which the high-frequency gain of the plant was assumed positive. In this paper, it is assumed that output disturbance in the plant exists and only the sign of the high-frequency gain

is known, which distinguishes the current work from the literature.

Consider the following state-space model of a general linear system with relative degree one.

$$\dot{\mathbf{x}}_\mathrm{p} = \mathbf{A}_\mathrm{p}\mathbf{x}_\mathrm{p} + \mathbf{B}_\mathrm{p}u, \tag{1}$$

$$y_\mathrm{p} = \mathbf{C}_\mathrm{p}^\mathrm{T}\mathbf{x}_\mathrm{p} + d, \tag{2}$$

where $\mathbf{x}_\mathrm{p} : \mathbb{R}^+ \to \mathbb{R}^n$ is the state vector, $u : \mathbb{R}^+ \to \mathbb{R}$ denotes the input, $d : \mathbb{R}^+ \to \mathbb{R}^n$ is uniformly bounded disturbance and $y_\mathrm{p} : \mathbb{R}^+ \to \mathbb{R}$ indicates the output. $\{\mathbf{A}_\mathrm{p}, \mathbf{B}_\mathrm{p}, \mathbf{C}_\mathrm{p}\}$ are observable and controllable. The transfer function of (1)-(2) is given as follows:

$$G_\mathrm{p}(s) = k_\mathrm{p}\frac{Z_\mathrm{p}(s)}{R_\mathrm{p}(s)} = \mathbf{C}_\mathrm{p}^\mathrm{T}(s\mathbf{I} - \mathbf{A}_\mathrm{p})^{-1}\mathbf{B}_\mathrm{p}, \tag{3}$$

where $s$ is the Laplace variable, $k_p$ is the high-frequency gain of the system, $Z_\mathrm{p}(s)$ and $R_\mathrm{p}(s)$ are polynomials of degrees $n-1$ and $n$, respectively. Assume that i) $Z_\mathrm{p}(s)$ is a Hurwitz polynomial and ii) $\mathrm{sgn}(k_\mathrm{p})$ is known.

A reference model is introduced as follows:

$$\dot{\mathbf{x}}_\mathrm{m} = \mathbf{A}_\mathrm{m}\mathbf{x}_\mathrm{m} + \mathbf{B}_\mathrm{m}r, \tag{4}$$

$$y_\mathrm{m} = \mathbf{C}_\mathrm{m}^\mathrm{T}\mathbf{x}_\mathrm{m}, \tag{5}$$

where $\mathbf{x}_\mathrm{m} : \mathbb{R}^+ \to \mathbb{R}^n$ indicates the state vector, $y_\mathrm{m} : \mathbb{R}^+ \to \mathbb{R}$ is the output, and $r : \mathbb{R}^+ \to \mathbb{R}$ denotes the reference signal. The transfer function of (4)-(5) is obtained as follows:

$$G_\mathrm{m}(s) = k_\mathrm{m}\frac{Z_\mathrm{m}(s)}{R_\mathrm{m}(s)}, \tag{6}$$

where $Z_\mathrm{m}(s)$ and $R_\mathrm{m}(s)$ are monic Hurwitz polynomials of degrees $n-1$ and $n$, respectively. Let $k_\mathrm{m}$ be positive and $G_\mathrm{m}(s)$ be a strictly positive real transfer function.

Now, the control law is defined as follows:

$$u = \hat{\boldsymbol{\theta}}^\mathrm{T}\boldsymbol{\phi}, \tag{7}$$

$$\hat{\boldsymbol{\theta}} = \left[\hat{k} \;\; \hat{\boldsymbol{\theta}}_1^\mathrm{T} \;\; \hat{\theta}_0 \;\; \hat{\boldsymbol{\theta}}_2^\mathrm{T}\right]^\mathrm{T}, \tag{8}$$

$$\boldsymbol{\phi} = \left[r \;\; \boldsymbol{\phi}_1^\mathrm{T} \;\; y_\mathrm{p} \;\; \boldsymbol{\phi}_2^\mathrm{T}\right]^\mathrm{T}, \tag{9}$$

where $\hat{k}$, $\hat{\theta}_0 : \mathbb{R}^+ \to \mathbb{R}$ and $\hat{\boldsymbol{\theta}}_1$, $\hat{\boldsymbol{\theta}}_2 : \mathbb{R}^+ \to \mathbb{R}^{n-1}$ are the estimated control parameters and $\boldsymbol{\phi}_1, \boldsymbol{\phi}_2 : \mathbb{R}^+ \to \mathbb{R}^{n-1}$ are the filtered signals from $u$ and $y_\mathrm{p}$, respectively, obtained by the following differential equations.

$$\dot{\boldsymbol{\phi}}_1 = \boldsymbol{\Lambda}\boldsymbol{\phi}_1 + \mathbf{b}u, \tag{10}$$

$$\dot{\boldsymbol{\phi}}_2 = \boldsymbol{\Lambda}\boldsymbol{\phi}_2 + \mathbf{b}y_\mathrm{p}, \tag{11}$$

where $\boldsymbol{\Lambda}$ is an asymptotically stable matrix. $\boldsymbol{\Lambda}$ and $\mathbf{b}$ are chosen so that $\det|s\mathbf{I} - \boldsymbol{\Lambda}| = Z_\mathrm{m}(s)$ and $(\boldsymbol{\Lambda}, \mathbf{b})$ is controllable. Let the vector $\boldsymbol{\theta}^* = [k^* \;\; \boldsymbol{\theta}_1^{*\mathrm{T}} \;\; \theta_0^* \;\; \boldsymbol{\theta}_2^{*\mathrm{T}}]^\mathrm{T}$ be the nominal parameter values such that if $\hat{\boldsymbol{\theta}} = \boldsymbol{\theta}^*$ the transfer function of the closed-loop system $G_0(s)$ under (7) matches the transfer function of the reference model $G_\mathrm{m}(s)$. Fig. 3 illustrates the overall control scheme discussed above.

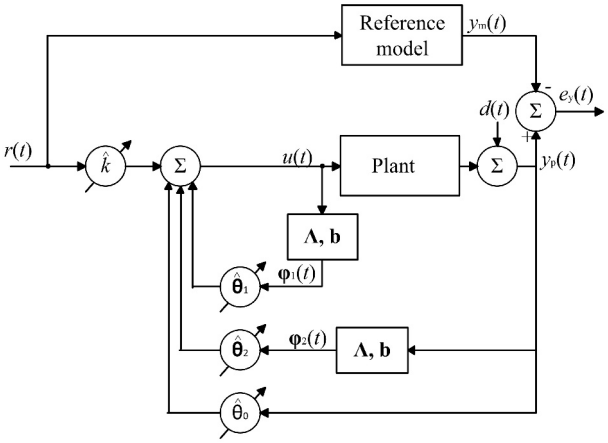


Fig. 3. Adaptive control scheme [23]: Output disturbance exists.

**Lemma** [39]**:** Consider the system $\dot{\mathbf{x}} = f(\mathbf{x})$ where $\mathbf{x} : \mathbb{R}^+ \to \mathbb{R}^n$. Let $\Psi^\mathrm{c}$ is the complement set of the set $\Psi$ that is a bounded neighborhood of the origin and $V(\mathbf{x})$ is a scalar function with continuous partial derivatives in $\Psi^\mathrm{c}$. The boundedness of the solution of the system is assured if the following conditions hold.

$$\text{i) } V(x) > 0 \;\; \forall x \in \Psi^\mathrm{c}, \tag{12}$$

$$\text{ii) } \dot{V}(x) \le 0 \;\; \forall x \in \Psi^\mathrm{c}, \tag{13}$$

$$\text{iii) } \lim_{\|x\|\to\infty} V(x) = \infty. \tag{14}$$

Now, the objective of the control system design is to derive an adaptive control input $u$, so that the tracking error $e_\mathrm{y} = y_\mathrm{p} - y_\mathrm{m}$ is uniformly ultimately bounded in the presence of $d$.

**Theorem 1:** Consider the plant in (1)-(2) and the reference model in (4)-(5) with transfer functions given by (3) and (6), respectively, and the control law in (7). Let the adaptation law be given by

$$\dot{\hat{\boldsymbol{\theta}}} = -\mathrm{sgn}(k_\mathrm{p})e_\mathrm{y}\boldsymbol{\phi} - \sigma\hat{\boldsymbol{\theta}}, \tag{15}$$

where $\sigma$ is a positive constant. Then the tracking error $e_\mathrm{y} = y_\mathrm{p} - y_\mathrm{m}$ and the parameter errors $\tilde{\boldsymbol{\theta}} = \hat{\boldsymbol{\theta}} - \boldsymbol{\theta}^*$ are bounded for any bounded initial conditions. Furthermore, there exists a set $\Psi$ that has a bounded neighborhood of the origin $(e_\mathrm{y}, \tilde{\boldsymbol{\theta}}) = (0,0)$ such that every $e_\mathrm{y}$ and $\tilde{\boldsymbol{\theta}}$ starting outside of $\Psi$ enter $\Psi$ at a finite time, and remains in $\Psi$ after that time.

**Proof:** Substituting (7) and (2) into (1), (10), and (11) yields the following equations describing the closed-loop system.

$$\dot{\mathbf{x}}_\mathrm{p} = \mathbf{A}_\mathrm{p}\mathbf{x}_\mathrm{p} + \mathbf{B}_\mathrm{p}(\hat{\boldsymbol{\theta}}^\mathrm{T}\boldsymbol{\phi}), \tag{16}$$

$$\dot{\boldsymbol{\phi}}_1 = \boldsymbol{\Lambda}\boldsymbol{\phi}_1 + \mathbf{b}(\hat{\boldsymbol{\theta}}^\mathrm{T}\boldsymbol{\phi}), \tag{17}$$

$$\dot{\boldsymbol{\phi}}_2 = \boldsymbol{\Lambda}\boldsymbol{\phi}_2 + \mathbf{b}(\mathbf{C}_\mathrm{p}^\mathrm{T}\mathbf{x}_\mathrm{p} + d). \tag{18}$$

Using the definition of the parameter errors $\tilde{\boldsymbol{\theta}} = \hat{\boldsymbol{\theta}} - \boldsymbol{\theta}^* = \begin{bmatrix}\tilde{k} & \tilde{\boldsymbol{\theta}}_1^\mathrm{T} & \tilde{\theta}_0 & \tilde{\boldsymbol{\theta}}_2^\mathrm{T}\end{bmatrix}^\mathrm{T}$, the overall system can be rewritten as follows:

$$\dot{\mathbf{z}}_\mathrm{p} = \mathbf{A}_\mathrm{z}\mathbf{z}_\mathrm{p} + \mathbf{B}_\mathrm{z}(\tilde{\boldsymbol{\theta}}^\mathrm{T}\boldsymbol{\phi} + k^* r) + \mathbf{D}_\mathrm{z}, \tag{19}$$

$$y = \mathbf{C}_\mathrm{z}^\mathrm{T}\mathbf{z}_\mathrm{p} + d, \tag{20}$$

where $\mathbf{z}_\mathrm{p} : \mathbb{R}^+ \to \mathbb{R}^{3n-2}$,

$$\mathbf{z}_\mathrm{p} = \begin{bmatrix}\mathbf{x}_\mathrm{p} \\ \boldsymbol{\phi}_1 \\ \boldsymbol{\phi}_2\end{bmatrix},\ \mathbf{A}_\mathrm{z} = \begin{bmatrix}\boldsymbol{\Lambda} + \mathbf{B}_\mathrm{p}\theta_0^*\mathbf{C}_\mathrm{p} & \mathbf{B}_\mathrm{p}\boldsymbol{\theta}_1^{*T} & \mathbf{B}_\mathrm{p}\boldsymbol{\theta}_2^{*T} \\ \mathbf{b}\theta_0^*\mathbf{C}_\mathrm{p} & \boldsymbol{\Lambda} + \mathbf{b}\boldsymbol{\theta}_1^{*T} & \mathbf{b}\boldsymbol{\theta}_2^{*T} \\ \mathbf{b}\mathbf{C}_\mathrm{p} & 0 & \boldsymbol{\Lambda}\end{bmatrix},$$

$$\mathbf{B}_\mathrm{z} = \begin{bmatrix}\mathbf{B}_\mathrm{p} \\ \mathbf{b} \\ 0\end{bmatrix},\ \mathbf{C}_z = \begin{bmatrix}\mathbf{C}_\mathrm{p} \\ 0 \\ 0\end{bmatrix},\ \mathbf{D}_\mathrm{z} = \begin{bmatrix}0 \\ 0 \\ \mathbf{b}d\end{bmatrix}. \tag{21}$$

The closed-loop system is represented by a $(3n-2)$th order system (19)-(20). Since $G_0(s) = G_\mathrm{m}(s)$ when $\hat{\boldsymbol{\theta}} = \boldsymbol{\theta}^*$, the reference model is also described by the following $(3n-2)$th order system.

$$\dot{\mathbf{z}}_\mathrm{m} = \mathbf{A}_\mathrm{z}\mathbf{z}_\mathrm{m} + \mathbf{B}_\mathrm{z}k^* r, \tag{22}$$

$$y_\mathrm{m} = \mathbf{C}_\mathrm{z}^\mathrm{T}\mathbf{z}_\mathrm{m}. \tag{23}$$

The transfer function of (22)-(23) is obtained as follows:

$$G_\mathrm{m}(s) = k^*\mathbf{C}_\mathrm{z}^\mathrm{T}(s\mathbf{I} - \mathbf{A}_\mathrm{z})^{-1}\mathbf{B}_\mathrm{z}, \tag{24}$$

where $\mathbf{z}_\mathrm{m}$ is the state vector of the reference model, which corresponds to the state vector $\mathbf{z}_\mathrm{p}$ of (19). From (19)-(20) and (22)-(23), the state error $\mathbf{e} = \mathbf{z}_\mathrm{p} - \mathbf{z}_\mathrm{m}$ and the tracking error $e_\mathrm{y} = y_\mathrm{p} - y_\mathrm{m}$ are obtained as follows:

$$\dot{\mathbf{e}} = \mathbf{A}_\mathrm{z}\mathbf{e} + \mathbf{B}_\mathrm{z}(\tilde{\boldsymbol{\theta}}^\mathrm{T}\boldsymbol{\phi}) + \mathbf{D}_\mathrm{z}, \tag{25}$$

$$e_\mathrm{y} = \mathbf{C}_\mathrm{z}^\mathrm{T}\mathbf{e} + d. \tag{26}$$

In the case that $d = 0$, the adaptation law $\dot{\hat{\boldsymbol{\theta}}} = -\mathrm{sgn}(k_\mathrm{p})e_\mathrm{y}\boldsymbol{\phi}$ can be used to assure the boundedness of the tracking error $e_\mathrm{y}$. In the presence of an external disturbance $d$, the use of the mentioned adaptation law, however, can lead to unboundedness of the tracking error. Therefore, the modified adaptation law using the $\sigma$-modification scheme in (15) is used to handle the bounded disturbance. Since $G_\mathrm{m}(s)$ is strictly positive, the transfer function of (25)-(26) is also strictly positive. According to the Kalman-Yakubovich lemma, there exist two symmetric positive definite matrices $\mathbf{P}$ and $\mathbf{Q}$ satisfying

$$\mathbf{A}_\mathrm{z}^\mathrm{T}\mathbf{P} + \mathbf{P}\mathbf{A}_\mathrm{z} = -\mathbf{Q},$$
$$\mathbf{P}\mathbf{B}_\mathrm{z} = \mathrm{sgn}(k_\mathrm{p})\mathbf{C}_\mathrm{z}. \tag{27}$$

The following positive definite function is considered to verify the boundedness of the tracking error and the estimated parameters.

$$V(\mathbf{e}, \tilde{\boldsymbol{\theta}}) = \frac{1}{2}\mathbf{e}^\mathrm{T}\mathbf{P}\mathbf{e} + \frac{1}{2}\tilde{\boldsymbol{\theta}}^\mathrm{T}\tilde{\boldsymbol{\theta}}. \tag{28}$$

The time derivative of $V(\mathbf{e}, \hat{\boldsymbol{\theta}})$ is obtained as follows:

$$\dot{V}(\mathbf{e}, \tilde{\boldsymbol{\theta}}) = -\frac{1}{2}\mathbf{e}^\mathrm{T}\mathbf{Q}\mathbf{e} - \sigma\tilde{\boldsymbol{\theta}}^\mathrm{T}\tilde{\boldsymbol{\theta}} + \mathbf{e}^\mathrm{T}\mathbf{P}\mathbf{D}_\mathrm{z} - \tilde{\boldsymbol{\theta}}^\mathrm{T}\left(\sigma\boldsymbol{\theta}^* + sgn(k_\mathrm{p})d\boldsymbol{\phi}\right). \tag{29}$$

There exist the positive constants $\lambda_1$ depending on the matrix $\mathbf{Q}$ and $\lambda_2$ depending on the reference model and the bounded external reference signal such that $\|\boldsymbol{\phi}\| \le \|\mathbf{e}\| + \lambda_1$ and

$$\begin{aligned}\dot{V}(\mathbf{e}, \tilde{\boldsymbol{\theta}}) \le & -\lambda_1\|\mathbf{e}\|^2 - \sigma\left\|\tilde{\boldsymbol{\theta}}\right\|^2 + \|\mathbf{e}\|\|\mathbf{P}\mathbf{D}_\mathrm{z}\| \\ & + \left\|\tilde{\boldsymbol{\theta}}\right\|(\sigma\|\boldsymbol{\theta}^*\| + \lambda_2\|d\|) + \left\|\tilde{\boldsymbol{\theta}}\right\|\|d\|\|\mathbf{e}\| \\ \le & -\left[\frac{\lambda_1}{2}\|\mathbf{e}\|^2 - \frac{1}{2\sigma}(\sigma\|\boldsymbol{\theta}^*\| + \lambda_2\|d\|)^2 \right. \\ & \left. - \frac{\|\mathbf{P}\mathbf{D}_\mathrm{z}\|^2}{\lambda_1} + \left\|\tilde{\boldsymbol{\theta}}\right\|^2\left(\frac{\sigma}{2} - \frac{\|d\|^2}{\lambda_1}\right)\right] \\ & - \frac{\lambda_1}{4}\left(\|\mathbf{e}\| - \frac{2}{\lambda_1}\|\mathbf{P}\mathbf{D}_\mathrm{z}\|\right)^2 \\ & - \frac{\sigma}{2}\left(\left\|\tilde{\boldsymbol{\theta}}\right\| - \|\boldsymbol{\theta}^*\| - \frac{\lambda_1}{\sigma}\|d\|\right)^2 \\ & - \frac{\lambda_1}{4}\left(\|\mathbf{e}\| - \frac{2}{\lambda_1}\left\|\tilde{\boldsymbol{\theta}}\right\|\|d\|\right)^2.\end{aligned} \tag{30}$$

Inequality (30) shows that $\dot{V}(\mathbf{e}, \hat{\boldsymbol{\theta}}) \le 0$ outside the set $\Psi$, where the set $\Psi$ is defined as follows:

$$\begin{aligned}\Psi = & \left\{(\mathbf{e}, \tilde{\boldsymbol{\theta}}) : \frac{\lambda_1}{2}\|\mathbf{e}\|^2 + \left\|\tilde{\boldsymbol{\theta}}\right\|^2\left(\frac{\sigma}{2} - \frac{\|d\|^2}{\lambda_1}\right)\right. \\ & \left. \le \frac{\|\mathbf{P}\mathbf{D}_\mathrm{z}\|^2}{\lambda_1} + \frac{1}{2\sigma}(\sigma\|\boldsymbol{\theta}^*\| + \lambda_2\|d\|)^2\right\}.\end{aligned} \tag{31}$$

Since the disturbance term $\mathbf{D}_\mathrm{z}$ and $d$ are bounded, the boundedness of the set $\Psi$ is assured and hence $\mathbf{e}$ and $\tilde{\boldsymbol{\theta}}$ are bounded according to Lemma 1. Owing to the boundedness of $\mathbf{e}$, (26) reveals that the tracking error $e_\mathrm{y}$ is also bounded. Furthermore, $\Psi$ is a bounded neighborhood of the origin $(\mathbf{e}, \tilde{\boldsymbol{\theta}}) = (0, 0)$. Therefore, $\Psi$ is also a neighborhood of $(e_\mathrm{y}, \tilde{\boldsymbol{\theta}}) = (0, 0)$. According to (26) and (30), we conclude that every $e_\mathrm{y}$ and $\tilde{\boldsymbol{\theta}}$ starting outside of $\Psi$ enter $\Psi$ at a finite time and remain in $\Psi$ after that time. The proof is completed. □

## 3. APPLICATION TO THE CEDM IN NUCLEAR SYSTEMS

The solenoid system in the CEDM is modeled as an electromagnetic mechanical system, as shown in Fig. 2. As shown in this figure, the system includes an electrical circuit consisting of an inductor and a resistor, a magnetic circuit with air gaps, and a mass-spring-damper mechanism. When the inductor is energized, a magnetic force that acts to draw the plunger to the pole is generated.

Through a sequence of the energizing/de-energizing processes of the inductors of solenoid actuators in the CEDM, the amount of insertion of the control rods is adjusted. During the operation of the CEDM, the parameters of solenoid actuators vary depending on the environmental conditions and the operating level. Therefore, a control law that deals with uncertainties and the change of system parameters is very much desirable. The objective of this section is to develop an adaptive control law for controlling the energizing/de-energizing process of the inductors of solenoid actuators in the presence of unknown parameters and output disturbances.

### 3.1. Mathematical model

A simplified mathematical model of the solenoid system is developed based on Kirchhoff's voltage law and the magnetic co-energy theory. Also, the model is restricted by the following assumptions: i) The solenoid operates in the linear region of B/H magnetization curve of the material (i.e., the B/H curve is a plot that describes the relationship between the magnetic flux density B and the magnetic field intensity H; therefore, the saturation and hysteresis effects due to losses in the magnetic core are not considered), and ii) the flux leakage is negligible.

Under the above assumptions, the solenoid can be modeled by a resistor in series with a linear inductor (see Fig. 2). According to Kirchhoff's voltage law, the following differential equation describing the voltage/current relationship of the solenoid with the inductance $L(x)$ and the resistance $R$ is obtained:

$$v(t) = L(x)\frac{\mathrm{d}i(t)}{\mathrm{d}t} + i(t)\frac{\mathrm{d}L(x)}{\mathrm{d}x}\frac{\mathrm{d}x}{\mathrm{d}t} + Ri(t), \tag{32}$$

where $v(t)$ and $i(t)$ are the voltage input and the current output, respectively; $x$ denotes the displacement of the plunger.

The electrical equivalent circuit of the magnetic circuit is shown in Fig. 4(b), where $F_\mathrm{m}$ is the magneto-motive force, $\Phi$ denotes the magnetic flux of the magnetic circuit, and $R_1$, $R_2$, $R_3$, and $R_4$ are the reluctance of the pole, the main air gap, the plunger, and the secondary air gap, respectively. The magneto-motive force, which represents the ability to create a magnetic flux in the magnetic circuit, is defined as follows:

$$F_\mathrm{m} = Ni(t) = \Phi R_\mathrm{m}, \tag{33}$$

where $N$ is the number of turns in the inductor, and $R_\mathrm{m}$ denotes the total reluctance of the magnetic circuit. From the magnetic point of view, the inductance of the solenoid is given as

$$L(x) = \frac{N\Phi}{i(t)}. \tag{34}$$

Substituting (33) into (34) yields

$$L(x) = \frac{N^2}{R_\mathrm{m}}. \tag{35}$$

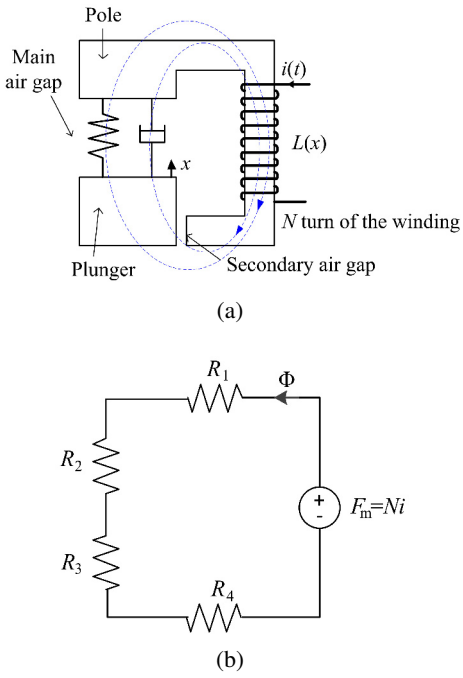


Fig. 4. (a) Magnetic circuit of the solenoid system, (b) electrical equivalent circuit of the magnetic circuit.

As the permeability of the pole and plunger material (i.e., electromagnetic material) is more significant than the permeability of the free space, the pole and plunger reluctances are negligible. The total reluctance $R_\mathrm{m}$, therefore, can be regarded as the summation of $R_2$ and $R_4$, which is given as follows:

$$R_\mathrm{m} = R_2 + R_4 = \frac{l_0 - x}{\mu_0 A_\mathrm{m}} + \frac{\delta}{\mu_0 A_\mathrm{s}}, \tag{36}$$

where $l_0$ is the initial main air gap length, $\delta$ denotes the secondary air gap length, $A_\mathrm{m}$ and $A_\mathrm{s}$ are the main and secondary air gap areas where the flux is crossing, respectively, and $\mu_0$ indicates the permeability of the free space. Substituting (36) into (35), the inductance can be rewritten as follows:

$$L(x) = \frac{N^2}{\frac{l_0 - x}{\mu_0 A_\mathrm{m}} + \frac{\delta}{\mu_0 A_\mathrm{s}}} = \frac{\mu_0 A_\mathrm{m} A_\mathrm{s} N^2}{(l_0 - x)A_\mathrm{s} + \delta A_\mathrm{m}}. \tag{37}$$

The derivative of the inductance with respect to $x$ is calculated as follows:

$$\begin{aligned}\frac{\mathrm{d}L(x)}{\mathrm{d}x} &= \frac{\mathrm{d}}{\mathrm{d}x}\left[\frac{\mu_0 A_\mathrm{m} A_\mathrm{s} N^2}{(l_0 - x)A_\mathrm{s} + \delta A_\mathrm{s}}\right] \\ &= \frac{\mu_0 A_\mathrm{m} A_\mathrm{s}^2 N^2}{[(l_0 - x)A_\mathrm{s} + \delta A_\mathrm{m}]^2} \\ &= \frac{1}{\mu_0 A_\mathrm{m} N^2}\left[\frac{\mu_0 A_\mathrm{m} A_\mathrm{s} N^2}{(l_0 - x)A_\mathrm{s} + \delta A_\mathrm{m}}\right]^2 \\ &= \frac{L(x)^2}{\mu_0 A_\mathrm{m} N^2}.\end{aligned} \tag{38}$$

Based on the co-energy theory in which there is no energy loss, and all the electric energy is stored as electromagnetic energy in the core, the electromagnetic force $F$ is derived as follows:

$$F = \frac{\partial W_{\mathrm{e}}(i,x)}{\partial x}, \tag{39}$$

where $W_{\mathrm{e}}(i,x)$ is the electromagnetic energy, whose formula is given, based on the co-energy theory, as follows:

$$W_{\mathrm{e}}(i,x) = \frac{1}{2}L(x)i(t)^2. \tag{40}$$

From (38)-(40), the electromagnetic force produced by the electromagnetic circuit is calculated as follows:

$$F = \frac{1}{2}\frac{L(x)^2}{\mu_0 A_{\mathrm{m}}}i(t)^2. \tag{41}$$

The main purpose of this section is to establish a simplified model of the solenoid system for designing a force controller. Therefore, it is assumed that the plunger has reached the desired position and is supposed to exert the force; namely, the displacement of the plunger is considered as a constant. Therefore, the voltage/current relationship (32) and the current/force relationship (41) can be simplified as follows:

$$v(t) = L\frac{\mathrm{d}i(t)}{\mathrm{d}t} + Ri(t), \tag{42}$$

$$F = \frac{1}{2}\frac{L^2}{\mu_0 A_{\mathrm{m}}}i(t)^2. \tag{43}$$

It is observed that the voltage/current relationship is characterized by a linear first-order differential equation (42), whereas the force $F$ is related to the current $i(t)$ by the nonlinear algebraic function (43).

### 3.2. System identification

In practice, the solenoid operates under the presence of the saturation and hysteresis effects; hence, the coil inductance of the solenoid is nonlinear. Dynamic analysis and control of the nonlinear solenoid model, however, is somewhat involved. Therefore, this paper proposes the use of the linear model in the design of an adaptive controller. The mathematical model of a known structure is determined through model identification using experimental input/output data of the upper lift coil. The prediction error method (PEM) [40, 41] for the linear model, which is a conventional identification technique, is used to estimate the solenoid model.

According to the PEM, the model is considered as the following predictor of the next output.

$$\hat{i}(t) = f\left(Z_{t-1}\right), \tag{44}$$

where $\hat{i}(t)$ denotes the one-step ahead prediction of the output current, $Z_{\mathrm{T}} = \{v(1),\ i(1),\ v(2),\ i(2),\ \ldots,\ v(T),\ i(T)\}$ is an observed data set which collects all past input and output data up to time T, and $f$ is an arbitrary function. Although the experimental input voltage and output current data are sampled at discrete time points, it still handles the continuous-time model well. The predictor is then parameterized in terms of a parameter vector $\boldsymbol{\Theta}$, namely,

$$\hat{i}(t) = f\left(\boldsymbol{\Theta}, Z_{t-1}\right). \tag{45}$$

Subsequently, the estimated vector $\hat{\boldsymbol{\Theta}}$ of $\boldsymbol{\Theta}$ is derived based on (45) and $Z_{\mathrm{T}}$, such that the distances between $\hat{i}(1)$, $\hat{i}(2)$, $\ldots$, $\hat{i}(\mathrm{T})$ and $i(1)$, $i(2)$, $\ldots$, $i(\mathrm{T})$ are minimized in an appreciate norm.

Fig. 5 shows the results of system identification using the input generated by mixing different quadrature waveforms. The responses of six different estimated models are compared with the experimental output data. Fig. 5(a) reveals that the linear 1st-order model, which is the simplified dynamic model in (42), cannot describe the system dynamics correctly. System estimations using the linear 2nd, 3rd, and 4th-order models without zero have also shown similar results (i.e., Fig. 5(b), Fig. 5(c), and Fig. 5(d), respectively). Fig. 5(e) showed that the linear 3rd-order model with two zeros is relatively suitable for capturing system dynamics besides the nonlinear model (Fig. 5f). Furthermore, the design of a controller using the linear model, nonetheless, leads to mathematical simplicity. Therefore, the linear 3rd-order model with three poles and two zeros, which is shown below, is used for developing the controller.

$$\dddot{i} + a_1\ddot{i} + a_2\dot{i} + a_3 i = k_{\mathrm{p}}\left(\ddot{v} + b_1\dot{v} + b_2\right), \tag{46}$$

where $a_1$, $a_2$, $a_3$, $k_{\mathrm{p}}$, $b_1$, and $b_2$ are unknown parameters, $\dot{(\cdot)}$ denotes the derivative with respect to time. The arguments of $i(t)$ and $v(t)$ are also simplified by $i$ and $v$.

### 3.3. Control law

As mentioned in Section 3.1, the force signal can be converted to the current signal via the nonlinear algebraic function (43). Therefore, the design of a force controller for the upper lift coil can be considered as the design of a current controller. The linear model (46) is used to apply MRAC, and the unmodeled dynamics are considered as the error between the reference model and the real model.

The solenoid model (46) under the output disturbance $d$ can be transformed to the following controllable canonical form.

$$\dot{\mathbf{x}}_{\mathrm{p}} = \mathbf{A}_{\mathrm{p}}\mathbf{x}_{\mathrm{p}} + \mathbf{B}_{\mathrm{p}}v, \tag{47}$$

$$i = \mathbf{C}_{\mathrm{p}}^{\mathrm{T}}\mathbf{x}_{\mathrm{p}} + d, \tag{48}$$

where $\mathbf{x}_{\mathrm{p}} : \mathbb{R}^+ \to \mathbb{R}^3$,

$$\mathbf{A} = \begin{bmatrix} 0 & 1 & 0 \\ 0 & 0 & 1 \\ -a_3 & -a_2 & -a_1 \end{bmatrix},\ \mathbf{B} = \begin{bmatrix} 0 \\ 0 \\ 1 \end{bmatrix},\ \mathbf{C} = \begin{bmatrix} k_{\mathrm{p}} \\ k_{\mathrm{p}}b_1 \\ k_{\mathrm{p}}b_2 \end{bmatrix}. \tag{49}$$

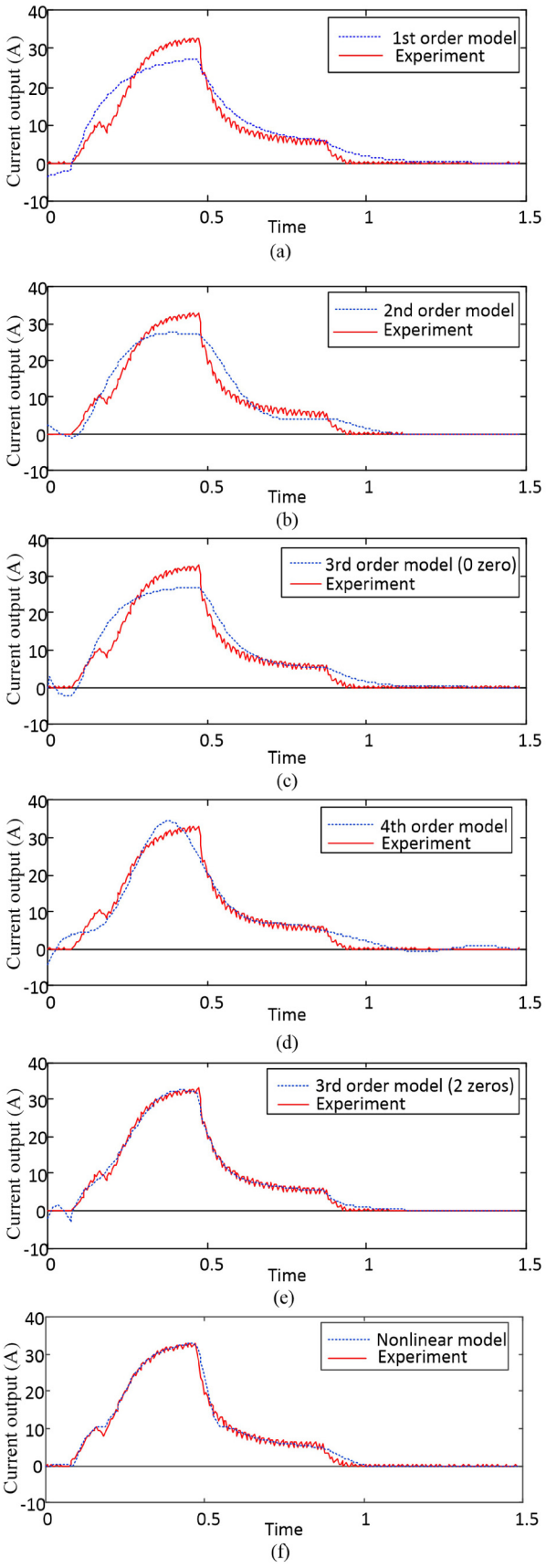


Fig. 5. System identification using PEM.

The transfer function of the solenoid system is shown as follows:

$$G_{\mathrm{p}}(s) = k_{\mathrm{p}} \frac{s^2 + b_1 s + b_2}{s^3 + a_1 s^2 + a_2 s + a_3}. \tag{50}$$

The transfer function of the associated 3rd-order reference model with the input/output pair $\{r(t), i_{\mathrm{m}}(t)\}$ is given by

$$G_{\mathrm{m}}(s) = k_{\mathrm{m}} \frac{s^2 + b_{1\mathrm{m}} s + b_{2\mathrm{m}}}{s^3 + a_{1\mathrm{m}} s^2 + a_{2\mathrm{m}} s + a_{3\mathrm{m}}}. \tag{51}$$

According to the theorem in Section 2, the control law $v$ and the adaptation law for the solenoid system are given as follows:

$$v = \hat{k} r + \hat{\theta}_{11}\phi_{11} + \hat{\theta}_{12}\phi_{12} + \hat{\theta}_0 e_{\mathrm{i}} + \hat{\theta}_{21}\phi_{21} + \hat{\theta}_{22}\phi_{22}, \tag{52}$$

and the adaptation laws

$$\dot{\hat{k}} = -\mathrm{sgn}(k_{\mathrm{p}}) e_{\mathrm{i}} r - \sigma \hat{k}, \tag{53}$$

$$\dot{\hat{\theta}}_0 = -\mathrm{sgn}(k_{\mathrm{p}}) e_{\mathrm{i}} i - \sigma \hat{\theta}_0, \tag{54}$$

$$\dot{\hat{\theta}}_{11} = -\mathrm{sgn}(k_{\mathrm{p}}) e_{\mathrm{i}} \phi_{11} - \sigma \hat{\theta}_{11}, \tag{55}$$

$$\dot{\hat{\theta}}_{12} = -\mathrm{sgn}(k_{\mathrm{p}}) e_{\mathrm{i}} \phi_{12} - \sigma \hat{\theta}_{12}, \tag{56}$$

$$\dot{\hat{\theta}}_{21} = -\mathrm{sgn}(k_{\mathrm{p}}) e_{\mathrm{i}} \phi_{21} - \sigma \hat{\theta}_{21}, \tag{57}$$

$$\dot{\hat{\theta}}_{22} = -\mathrm{sgn}(k_{\mathrm{p}}) e_{\mathrm{i}} \phi_{22} - \sigma \hat{\theta}_{22}, \tag{58}$$

$$\begin{bmatrix} \dot{\phi}_{11} \\ \dot{\phi}_{12} \end{bmatrix} = \mathbf{\Lambda} \begin{bmatrix} \phi_{11} \\ \phi_{12} \end{bmatrix} + \mathbf{b} v, \tag{59}$$

$$\begin{bmatrix} \dot{\phi}_{21} \\ \dot{\phi}_{22} \end{bmatrix} = \mathbf{\Lambda} \begin{bmatrix} \phi_{21} \\ \phi_{22} \end{bmatrix} + \mathbf{b} i_{\mathrm{p}}, \tag{60}$$

where $e_{\mathrm{i}} = i - i_{\mathrm{m}}$, $\mathbf{\Lambda}$ is a $2 \times 2$ asymptotically stable matrix, and $\mathbf{b}$ is a $2 \times 1$ vector. Furthermore, $\det|s\mathbf{I} - \mathbf{\Lambda}| = s^2 + b_{1\mathrm{m}} s + b_{2\mathrm{m}}$ and $(\mathbf{\Lambda}, \mathbf{b})$ is controllable.

## 4. SIMULATION RESULTS

In this section, the simulations are carried out to verify the performance of the modified MRAC. The responses of the upper lift coil under the designed control law are shown and compared with those under the following PI control law. $v(t) = K_{\mathrm{P}} e(t) + K_{\mathrm{I}} \int_0^t e(\tau) d\tau$, where $K_{\mathrm{P}} = 2$ and $K_{\mathrm{I}} = 0.6$. The reference current is generated to withdraw and hold control rods. In detail, the current is increased to a threshold value to produce a magnetic force drawing plunger (i.e., the draw phase); after reaching the threshold value, the current is reduced to a lower value, which is sufficient to maintain a holding force (i.e., the holding phase).

Fig. 6 shows the current output of the system using the PI control (see Fig. 6(a)) and the modified MRAC control (Fig. 6(b)) in the normal condition. In this state, it is assumed that the plant parameters are known. This reveals that the performances of two controllers are not noticeable except the fact that the modified MRAC takes a short

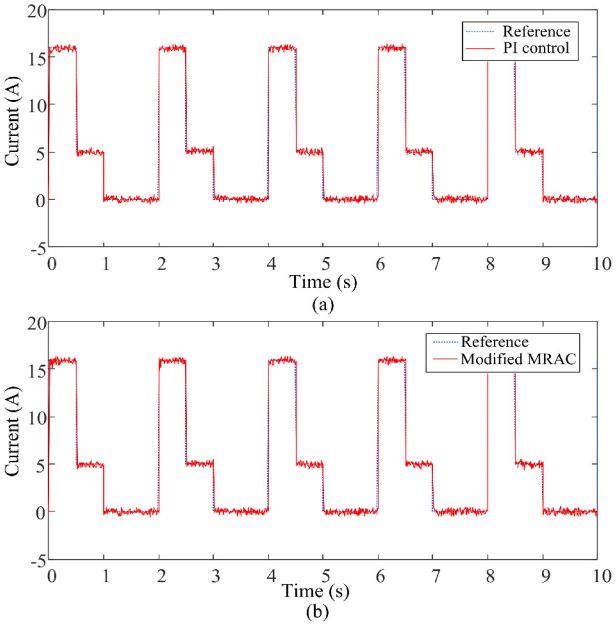


Fig. 6. Comparison of the responses in the normal state: (a) PI control, (b) the proposed MRAC.

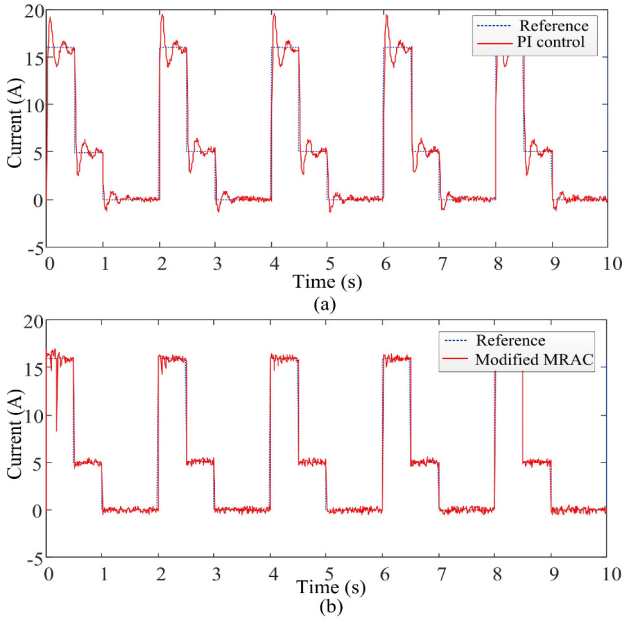


Fig. 7. Comparison of the responses in the abnormal state: (a) PI control, (b) the proposed MRAC.

time to adjust the control parameters. For PI control, the error between the output current and the reference current is smaller than the modified MRAC control due to well-tuned control parameters $K_{\mathrm{I}}$ and $K_{\mathrm{P}}$ for known plant parameters. The responses of the overall closed-loop system in the abnormal condition are demonstrated in Fig. 7. In this state, the plant parameters are changed and not known due to external factors. The results show that the performance of the PI control is not good (Fig. 7(a)). While the response of the system using the modified MRAC still follows the reference current well after a short time to adjust the control parameters (Fig. 7(b)). The robustness of the modified MRAC is also compared with the conventional MRAC in Fig. 8. Under the output disturbance, the tracking error of the system using the modified MRAC is bounded above by $[-1.5, 1.5]$ (i.e., Fig. 8(a)). The simulation results validated that the designed control law can be used to control solenoid actuators of the CEDM in the nuclear system.

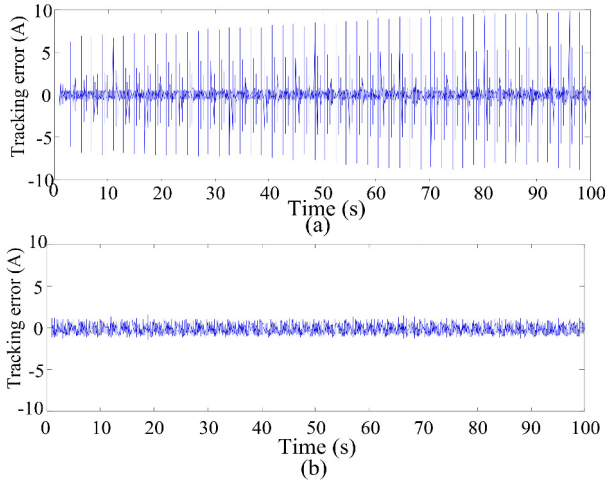


Fig. 8. Tracking errors: (a) Conventional MRAC, (b) the proposed MRAC.

## 5. EXPERIMENTAL RESULTS

The performance of the modified MRAC was verified experimentally. A testbed used to drive the CEDM mock-up is shown in Fig. 9, wherein the power supply consists of R/L load bank, 3 phase power, DC hold cabinet, power cabinet, power control unit, and oscilloscope.

The output currents of the upper lift coil (UL) in the withdrawal and insertion processes are demonstrated in Fig. 10 and Fig. 11, respectively. The conventional PI control shows limitations under the abnormal condition. The output current cannot be reached at the threshold value.

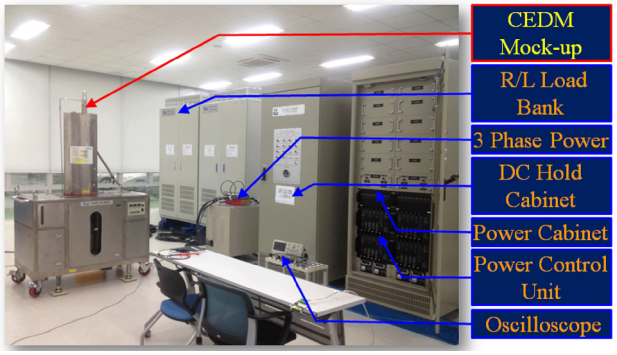


Fig. 9. Testbed used to drive the CEDM mock-up.

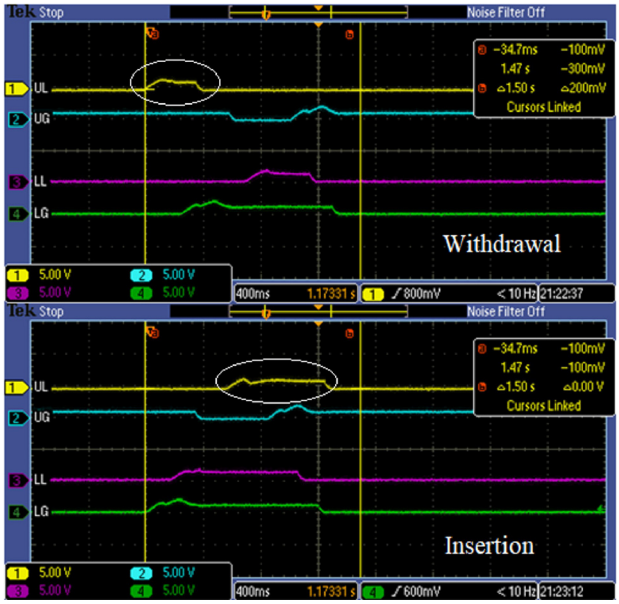


Fig. 10. Experimental results of a well-tuned PI controller in the abnormal condition.

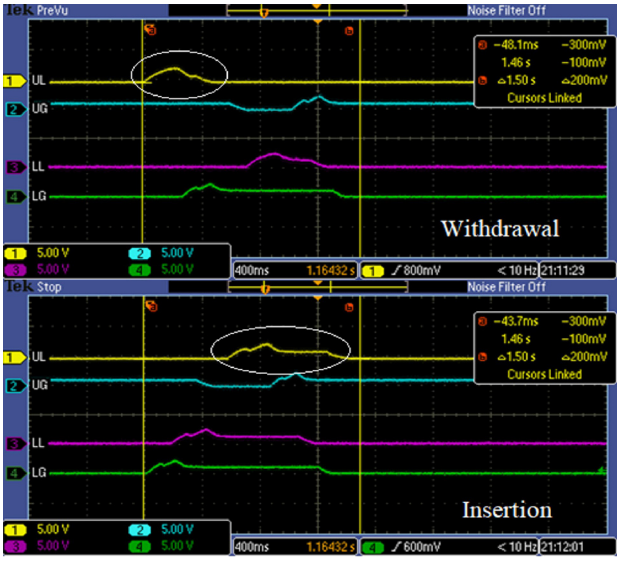


Fig. 11. Experimental results of the proposed MRAC in the abnormal condition.

With the PI control, it was impossible to move the CEDM in the abnormal condition accurately (i.e., see Fig. 10). On the other hand, the results in the response of the system under the MRAC are improved, as shown in Fig. 11. It shows that the solenoid actuators under the MRAC can move the CEDM properly regardless of external environmental or system-parametric changes.

## 6. CONCLUSION

A first-order linear model describing the simplified relationship between the input voltage and the magnetic force was developed using Kirchhoff's voltage law and the magnetic co-energy theory. System identification using the experimental input/output data showed that the first-order model is not suitable to predict the system behaviors compared to the third-order model with two zeros. Based on the third-order linear model, a robust control law was designed for current control of the solenoid actuator under the output disturbance based on the modified MRAC approach using the $\sigma$-modification scheme. The simulation and experiential results revealed that the proposed control law had achieved an excellent control performance when compared to the conventional PI control law, especially in the abnormal condition.

## REFERENCES

[1] K. J. Stambaugh, P. K. DeSantis, A. R. Mackovjak, and J. P. McLaughlin, "Control rod drive mechanism for nuclear reactor," United States Patent No. 8,811,561, Aug. 19, 2014.

[2] Y. Wu, Z. Chen, Z. Wang, S. Chen, D. Ge, C. Chen, J. Jia, Y. Li, M. Jin, T. Zhou, F. Wang, and L. Hu, "Nuclear safety in the unexpected second nuclear era," *Proceedings of the National Academy of Sciences*, vol. 116, no. 36, pp. 17673-17682, 2019.

[3] U. H. Shah and K.-S Hong, "Active vibration control of a flexible rod moving in water: Application to nuclear refueling machines," *Automatica*, vol. 93, 231-243, 2018.

[4] T. Ishida, S. Imayoshi, T. Yoritsune, H. Nunokawa, M. A. Ochiai, and Y. Ishizaka, "Development of in-vessel type control rod drive mechanism for marine reactor," *Journal of Nuclear Science and Technology*, vol. 38, no. 7, pp. 557-570, 2001.

[5] T. Yoritsune, T. Ishida, and S. Imayoshi, "In-vessel type control rod drives mechanism using magnetic force latching for a very small reactor," *Journal of Nuclear Science and Technology*, vol. 39, no. 8, pp. 913-922, 2002.

[6] J. S. Lee, S. S. Cho, and J. W. Kim, "Study on rod position indication system using permanent magnets with shielding plates for a control rod drive mechanism," *Journal of Magnetics*, vol. 20, no. 4, pp. 439-443, 2015.

[7] J. S. Lee, G. M. Lee, and J. W. Kim, "Design optimization of CRDM motor housing," *Journal of Magnetics*, vol. 21, no. 4, pp. 586-592, 2016.

[8] H. M. Kim, I. Y. Kim, and I. K. Kim, "Electromagnetic analysis of the magnetic jack type control element drive mechanism," *Proc. of the 17th International Conf. on Structural Mechanics in Reactor Technology*, Paper no. O03-7, 2003.

[9] J. Lee, H. Jun, and Y. Youn, "Experimental study of an electromagnetic actuator for a control element drive mechanism," *IEEE Trans. on Magnetics*, vol. 50, no. 11, pp. 1-4, 2014.

[10] N. D. Vaughan and J. B. Gamble, "The modeling and simulation of a proportional solenoid valve," *Journal of Dynamic Systems, Measurement, and Control*, vol. 118, no. 1, pp. 120-125, 1996.

[11] J. G. Zhang, H. J. Yian, Y. Q. Wu, X. X. Wu, S. Y. Yu, and S. Y. He, "Research on the electromagnetic structure of movable coil electromagnet drive mechanism for reactor control rod," *Journal of Nuclear Science and Technology*, vol. 44, no. 2, pp. 163-170, 2007.

[12] A. Dell'Amico and P. Krus, "Modelling and experimental validation of a nonlinear proportional solenoid pressure control valve," *International Journal of Fluid Power*, vol. 17, no. 2, pp. 90-101, 2016.

[13] M. Hosseini, S. Arzanpour, F. Golnaraghi, and A. M. Parameswaran, "Solenoid actuator design and modeling with application in engine vibration isolators," *Journal of Vibration and Control*, vol. 19, no. 7, pp. 1015-1023, 2013.

[14] M. F. Rahman, N. C. Cheung, and K. W. Lim, "Position estimation in solenoid actuators," *IEEE Trans. on Industry Applications*, vol. 32, no. 3, pp. 552-559, 1996.

[15] S. Butzmann, J. Melbert, and A. Koch, "Sensorless control of electromagnetic actuators for variable valve train," *SAE Transactions*, vol. 109, no.3, pp. 1425-1430, 2000.

[16] F. Ronchi, C. Rossi, and A. Tilli, "Sensing device for camless engine electromagnetic actuators," *Proceedings of the IEEE IECON 02*, vol. 2, pp. 1669-1674, 2002.

[17] R. Koch, A. F. Lynch, and R. R. Chladny, "Modeling and control of solenoid valves for internal combustion engines," *IFAC Proc. Volumes*, vol. 35, no. 2, pp. 197-202, 2002.

[18] M. Montanari, F. Ronchi, C. Rossi, and A. Tonielli, "Control of a camless engine electromechanical actuator: position reconstruction and dynamic performance analysis," *IEEE Trans. on Industrial Electronics*, vol. 51, no. 2, pp. 299-311, 2004.

[19] P. Eyabi and G. Washington, "Modeling and sensorless estimation for single spring solenoids," *Studies*, vol. 2013, pp. 08-14, 2006.

[20] S. Nagai, T. Nozaki, and A. Kawamura, "Environmental robust position control for compact solenoid actuators by sensorless simultaneous estimation of position and force," *IEEE Trans. on Industrial Electronics*, vol. 63, no. 8, pp. 5078-5086, 2016.

[21] K. S. Narendra and L. S. Valavani, "Stable adaptive controller design–direct control," *IEEE Trans. on Automatic Control*, vol. 23, no. 4, pp. 570-583, 1978.

[22] K. S. Narendra and L. S. Valavani, "Direct and indirect model reference adaptive control," *Automatica*, vol. 15, no. 6, pp. 653-664, 1979.

[23] K. S. Narendra and A. M. Annaswamy, *Stable Adaptive Systems*, Prentice Hall, New Jersey, 1989.

[24] Q. C. Nguyen, M. Piao, and K.-S. Hong, "Multivariable adaptive control of the rewinding process of a roll-to-roll system governed by hyperbolic partial differential equations," *International Journal of Control, Automation and Systems*, vol. 16, no. 5, pp. 2177-2186, 2018.

[25] Q. H. Ngo, K. S. Hong, and I. H. Jung, "Adaptive control of an axially moving system," *Journal of Mechanical Science and Technology*, vol. 23, no. 11, pp. 3071-3078, 2009.

[26] K.-S. Hong and P.-T. Pham, "Control of axially moving systems: A review," *International Journal of Control, Automation and Systems*, vol. 17, no. 12, pp. 2983-3008, 2019.

[27] S. Larguech, S. Aloui, O. Pagés, A. El Hajjaji, and A. Chaari, "Robust adaptive controller for the diesel engine air path with input saturation," *International Journal of Control, Automation and Systems*, vol. 17, no. 10, pp. 2541-2549, 2019.

[28] S. Ahmed, H. Wang, M. S. Aslam, I. Ghous, and I. Qaisar, "Robust adaptive control of robotic manipulator with input time-varying delay," *International Journal of Control, Automation and Systems*, vol. 17, no. 9, pp. 2193-2202, 2019.

[29] G. H. Kim and K.-S. Hong, "Adaptive sliding mode control of an offshore container crane with unknown disturbances," *IEEE/ASME Transactions on Mechatronics*, vol. 24, no. 6, pp. 2850-2861, 2019.

[30] O. Doukhi and D. J. Lee, "Neural network-based robust adaptive certainty equivalent controller for quadrotor UAV with unknown disturbances," *International Journal of Control, Automation and Systems*, vol. 17, no. 9, pp. 2365-2374, 2019.

[31] R. Wu, and J. Du, "Adaptive robust course-tracking control of time-varying uncertain ships with disturbances," *International Journal of Control, Automation and Systems*, vol. 17, no. 7, pp. 1847-1855, 2019.

[32] Y. Wang, K. Li, K. Yang, and H. Ji, "Adaptive backstepping control for spacecraft rendezvous on elliptical orbits based on transformed variables model," *International Journal of Control, Automation and Systems*, vol. 16, no. 1, pp. 189-196, 2018.

[33] K.-S. Hong, H. C. Sohn, and J. K. Hedrick, "Modified skyhook control of semi-active suspension: A new model, gain scheduling, and hardware-in-the-loop tuning," *Journal of Dynamic Systems, Measurement, and Control*, vol. 124, no. 1, pp. 158-167, 2002.

[34] Y. Tuo, Y. Wang, S. X. Yang, M. Biglarbegian, and M. Fu, "Robust adaptive dynamic surface control based on structural reliability for a turret-moored floating production storage and offloading vessel," *International Journal of Control, Automation and Systems*, vol. 16, no. 4, pp. 1648-1659, 2018.

[35] K.-S. Hong and J. Bentsman, "Direct adaptive control of parabolic systems: Algorithm synthesis, and convergence and stability analysis," *IEEE Trans. on Automatic Control*, vol. 39, no. 10, pp. 2018-2033, 1994.

[36] J. P. Dong, J. G. Sun, Y. Guo, and S. M. Song, "Suidance laws against towed decoy based on adaptive back-stepping sliding mode and anti-saturation methods," *International Journal of Control, Automation and Systems*, vol. 16, no. 4, pp. 1724-1735, 2018.

[37] S. D. Lee and S. Jung, "An adaptive control technique for motion synchronization by on-line estimation of a recursive least square method," *International Journal of Control, Automation and Systems*, vol. 16, no. 3, pp. 1103-1111, 2018.

[38] P. A. Ioannou and P. V. Kokotovic, *Adaptive Systems with Reduced Models*, Springer-Verlag, New York, 1983.

[39] J. P. LaSalle, "Some extensions of Liapunov's second method," *IRE Trans. on Circuit Theory*, vol. 7, pp. 520-527, 1960.

[40] L. Ljung, *System Identification–Theory for the User*, Prentice Hall, New Jersey, 2001.

[41] L. Ljung, "Prediction error estimation methods," *Circuits, Systems and Signal Processing*, vol. 21, no. 1, pp. 11-21, 2002.

**Bae-Jeong Park** received his B.S. degree in control engineering in 1998, and an M.S. degree in mechanical engineering in 2000, and pursues a doctoral degree for intelligent control and automation in the School of Mechanical Engineering, Pusan National University, Korea. He is currently working with the Nuclear I&C Control Systems Design Team of Doosan Heavy Industries and Construction. He is a Senior Engineer in charge of designing, verification, and validation of the Rod Control System in nuclear power plants. His research interests include input shaping control and adaptive control of electro-mechanical systems.

**Phuong-Tung Pham** received his B.S. and M.S degrees in mechanical engineering from Ho Chi Minh City University of Technology, in 2016 and 2018, respectively. He is currently a Ph.D. candidate in the School of Mechanical Engineering, Pusan National University, Korea. His research interests include nonlinear control, adaptive control, vibration control, and control of distributed parameter systems.

**Keum-Shik Hong** Please see vol. 17, no. 12, p. 3008, December, 2019 of this journal.